

MONTHLY WEATHER REVIEW

JAMES E. CASKEY, JR., Editor

Volume 85
Number 7

JULY 1957

Closed September 15, 1957
Issued October 15, 1957

PREDICTIVE CONSEQUENCES OF CERTAIN PHYSICAL INCONSISTENCIES IN THE GEOSTROPHIC BAROTROPIC MODEL

FREDERICK G. SHUMAN, U. S. Weather Bureau

Joint Numerical Weather Prediction Unit, Suitland, Md.

[Manuscript received June 7, 1957; revised July 22, 1957]

ABSTRACT

The physical inconsistency of geostrophic flow and small surface pressure tendencies is discussed. The frequently disastrous consequences in conventional geostrophic barotropic predictions are numerically identified by comparisons with experimental "semi-geostrophic" barotropic predictions from which the inconsistency has been removed. Effects of the inconsistency of the geostrophic wind field with the equations of motion are also quantitatively isolated by comparisons of semi-geostrophic predictions with predictions made with wind fields which satisfy the balance equation. It is concluded that the principal fault of the conventional geostrophic approximation lies in the violation of the continuity equation. Its lack of the dynamic effects expressed in the equations of motion seems also significant, but is less important.

1. INTRODUCTION

Conventional geostrophic barotropic 72-hour predictions were inaugurated on a daily basis by the Joint Numerical Weather Prediction (JNWP) Unit on September 29, 1955. The classic model of Charney [1] was the basis for the computations. Although not always present, the most consistent and characteristic error in these predictions was spurious anticyclogenesis, usually associated with flow around the western side of large subtropical Highs. Its maximum frequencies were over the southeastern coast of the United States, and in the central Pacific Ocean. Figure 3 is taken from a typical case when spurious anticyclogenesis was present over the former area.

2. THE IMPORTANCE OF THE LAW OF CONSERVATION OF MASS

The error is related to the divergence of the geostrophic wind, and can be traced to a particular physical inconsistency in the geostrophic barotropic model. For ease of reference the derivation of the model will be briefly reviewed here. A model equivalent barotropic atmosphere is first created in which

$$\begin{aligned}u &= A(p)u'(x, y) \\ v &= A(p)v'(x, y)\end{aligned}\tag{1}$$

where u and v are the two horizontal components of velocity.¹

The two horizontal equations of motion are integrated with respect to pressure, p , with the vertical convection terms neglected. The result in isobaric coordinates is

$$\begin{aligned}\bar{u}_t + K\bar{u}\bar{u}_x + K\bar{v}\bar{u}_y - f\bar{v} + g\bar{z}_x &= 0 \\ \bar{v}_t + K\bar{u}\bar{v}_x + K\bar{v}\bar{v}_y + f\bar{u} + g\bar{z}_y &= 0\end{aligned}\tag{2}$$

where f is the Coriolis parameter and g the acceleration of

¹ In order to avoid confusion in the following pages, it should be understood that equations (1), which represent the basic departure of the equivalent barotropic equations from the primitive meteorological equations are not, as they stand, inconsistent with the primitive equations. They are merely a statement of an instantaneous condition concerning the 3-dimensional distribution of wind velocities. An integration in time in which it is assumed that this condition is maintained is, of course, inconsistent with the primitive equations. This article will not deal with this physical inconsistency of the equivalent barotropic model when used as a predictive tool, nor will it deal with the validity of the concept of an equivalent barotropic level in the real atmosphere (Charney [1, 2]). In the calculations to be discussed, the equivalent barotropic level was taken to be at 500 mb., and the value of K , defined in equation (3), was set to unity.

gravity. The functions \bar{u} and \bar{v} are the values of u and v at the level \bar{p} where $A(p)$ is equal to its vertical pressure average; i. e.,

$$\bar{u} = A(\bar{p})u'$$

$$\bar{v} = A(\bar{p})v'$$

$$A(\bar{p}) = -p_0^{-1} \int_{p_0}^0 A(p) dp$$

The function, p_0 , is the pressure at the lower boundary. It is assumed to be constant, which is nearly true in the real atmosphere. The function, \bar{z} , is the vertical pressure average of the height, z , of isobaric surfaces; i. e.,

$$\bar{z} = -p_0^{-1} \int_{p_0}^0 z dp$$

The constant, K , is related to the shape of the vertical windspeed profile, and is defined as follows.

$$K = \frac{-p_0^{-1} \int_{p_0}^0 A^2 dp}{\left(-p_0^{-1} \int_{p_0}^0 A dp\right)^2} \quad (3)$$

The vorticity equation for the equivalent barotropic atmosphere is then derived from equations (2) by cross differentiation.

$$\bar{\zeta}_t + \bar{u}(K\bar{\zeta}_x + f_x) + \bar{v}(K\bar{\zeta}_y + f_y) + (K\bar{\zeta} + f)(\bar{u}_x + \bar{v}_y) = 0 \quad (4)$$

where $\bar{\zeta}$ is the relative vorticity,

$$\bar{\zeta} = \bar{v}_x - \bar{u}_y$$

The importance of physical consistency in the introduction of the geostrophic approximation to the wind may be seen at this point in the derivation. The divergence of the geostrophic wind is

$$(\bar{u}_x + \bar{v}_y)_g = -f^{-1}(\bar{u}_g f_x + \bar{v}_g f_y)$$

Thus, if one were to substitute from the geostrophic approximation into the vorticity equation (4), the Rossby term, $\bar{u}f_x + \bar{v}f_y$, would cancel, and the model could not properly account for the propagation of long westerly waves.

Proceeding with the derivation, we next introduce the equivalent barotropic continuity equation in the form of Margules' tendency equation.

$$\omega_0 = -p_0(\bar{u}_x + \bar{v}_y) \quad (5)$$

Where ω_0 is the substantial time derivative of pressure at the lower boundary. The vorticity equation (4) may then be written

$$\bar{\zeta}_t + \bar{u}(K\bar{\zeta}_x + f_x) + \bar{v}(K\bar{\zeta}_y + f_y) - (K\bar{\zeta} + f)p_0^{-1}\omega_0 = 0 \quad (6)$$

The next step has been to turn to the real atmosphere for two empirical facts. It has been noted that ω_0 is small, and that the wind is nearly geostrophic. These facts have been applied in the model by an omission of the last term in equation (6), and by a direct substitution into equation (6) from the geostrophic approximation,

$$-f\bar{v}_g + g\bar{z}_x = 0$$

$$+f\bar{u}_g + g\bar{z}_y = 0$$

Vanishing surface pressure tendencies and geostrophic winds, however, are physically inconsistent, for geostrophic flow would lead to large pressure tendencies at the lower boundary which could not be ignored. This can be made clear by a direct substitution from the geostrophic approximation into Margules' tendency equation (5). A light southerly mean wind of 10 knots would yield a value of ω_0 of 3 mb. hr.⁻¹ even at middle latitudes. The situation is worse at low latitudes, for with a given southerly wind component, geostrophic divergence varies as the cotangent of the latitude angle. Perspicacious neglect of the last term in equation (6) largely compensates for the direct substitution from the geostrophic approximation, otherwise the conventional geostrophic barotropic model would not predict as well as it does. Certain effects are not compensated, however.

In particular, the implied sink of vorticity in the convergence field of southerly geostrophic winds explains qualitatively the spurious anticyclogenesis exhibited in figure 3. If equation (4) is integrated over a region,

$$\iint \bar{\zeta} dx dy + \oint \bar{v}_n (K\bar{\zeta} + f) ds = 0$$

where \bar{v}_n is the wind component outward and normal to the boundary, and s is distance measured counter-clockwise along the boundary. Thus equation (4) implies that an increase of vorticity within a region equals the net transport of vorticity into the region across the boundary. The vorticity equation (4) is a statement of conservation in that sense.

Equation (6), on the other hand, if the last term is neglected, and if the geostrophic approximation to the wind is substituted, leads to

$$\iint \bar{\zeta} dx dy + \oint \bar{v}_n (K\bar{\zeta} + f) = - \iint (K\bar{\zeta} + f) f^{-1} (\bar{u}f_x + \bar{v}f_y) dx dy$$

The conventional geostrophic barotropic vorticity equation thus implies a vorticity sink in regions of southerly flow, and a vorticity source in regions of northerly flow. The strength of the source is related to the right-hand side of the preceding equation. Although initially (fig. 1) no pronounced southerly flow was evident over southern United States, any tendency toward development of southerly flow in the prediction would lead to creation of a sink of vorticity. It is not difficult to conceive of such

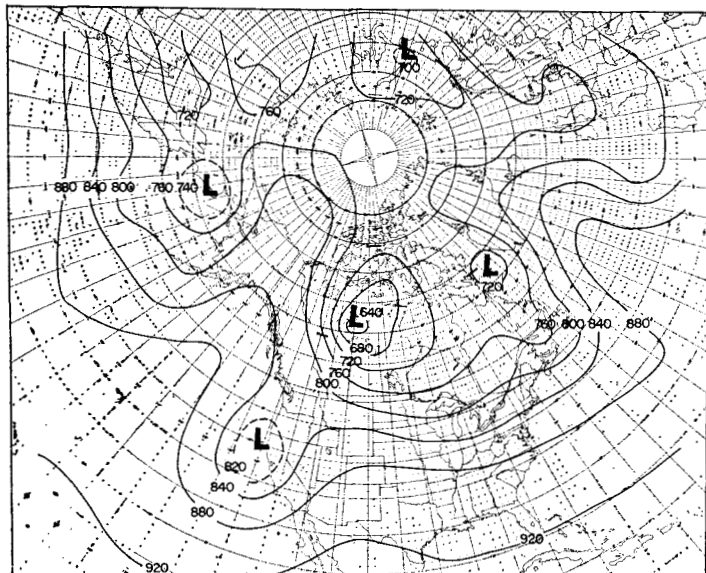


FIGURE 1.—Initial 500-mb. heights, 0300 GMT April 26, 1956. Contours are labeled in tens of feet.

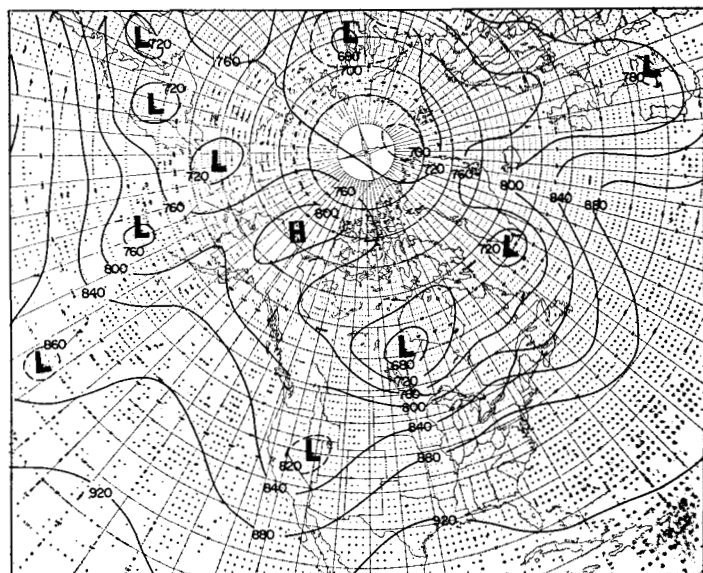


FIGURE 2.—Verifying 500-mb. heights for 36-hour forecasts, 1500 GMT April 27, 1956. Contours are labeled in tens of feet.

a sink “feeding back” to create more southerly flow, which in turn would strengthen the vorticity sink. It is just such a “feedback” mechanism which the author believes is directly responsible for the spurious anticyclone over South Carolina in figure 3.

It is incontrovertible that the conventional geostrophic barotropic model is physically inconsistent in the respect that it does not conserve mass. It is in order, therefore, to inquire into what errors arise from this physical inconsistency of the model, as opposed to other inconsistencies or to the lack of correspondence of the equivalent barotropic atmosphere (1) to the real atmosphere. One may make such an inquiry by devising a barotropic model in which the wind field is defined as very nearly geostrophic, but non-divergent. Such a model, which I shall call “semi-geostrophic barotropic,” does not violate the law of mass conservation for the classes of motion in which the surface pressure tendency is small or vanishing.

The geostrophic wind vector field shall be divided into an irrotational divergent part described by a velocity potential, S_1 , and a non-divergent rotational part described by a stream function, S_2 , in the expectation that the non-divergent part will closely approximate the geostrophic wind vector field, itself.

$$\mathbf{V}_g = -f^{-1}\nabla(gz) \times \mathbf{k} = \nabla S_1 - \nabla S_2 \times \mathbf{k} \quad (7)$$

where \mathbf{V}_g is the geostrophic wind velocity vector and \mathbf{k} is a unit vertical vector. The velocity potential, S_1 , does not appear in the curl of equation (7), while the stream function, S_2 , does not appear in the divergence of the equation.

$$\nabla \times \mathbf{V}_g \cdot \mathbf{k} = f^{-1}\nabla^2(gz) + \nabla(gz) \cdot \nabla f^{-1} = \nabla^2 S_2 \quad (8)$$

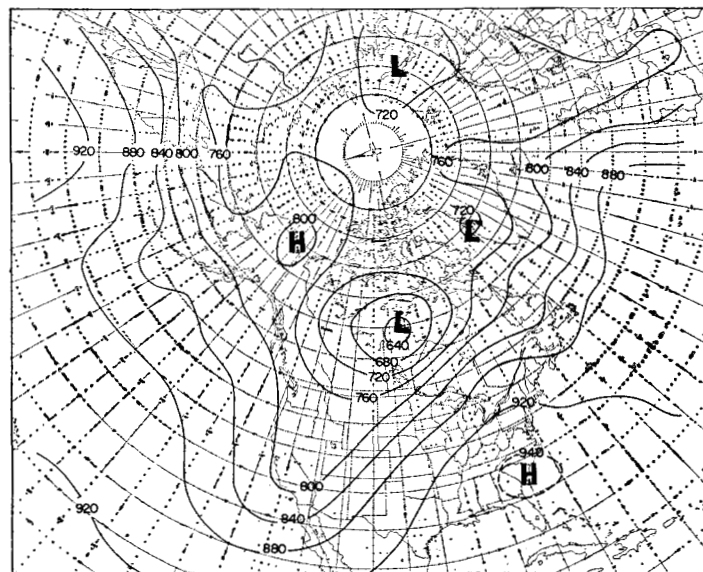


FIGURE 3.—A conventional geostrophic barotropic 36-hour prediction computed from initial conditions at 500 mb. at 0300 GMT April 26, 1956. Contours are labeled in tens of feet.

$$\nabla \cdot \mathbf{V}_g = J_{x,y}(gz, f^{-1}) = \nabla^2 S_1 \quad (9)$$

where $J_{x,y}$ is the Jacobian with respect to coordinates x, y . Since equations (8) and (9) are linear in the variables \mathbf{V}_g, S_1, S_2 , and z , the only variables appearing which depend on pressure, p , vertical pressure averages of the equations may be directly indicated by barring those variables. With the field of \bar{z} given as in figure 1, equation (8) was solved for S_2 . With the intention of making the non-divergent part of the wind component at and normal to the boundary nearly geostrophic, the boundary condition used was

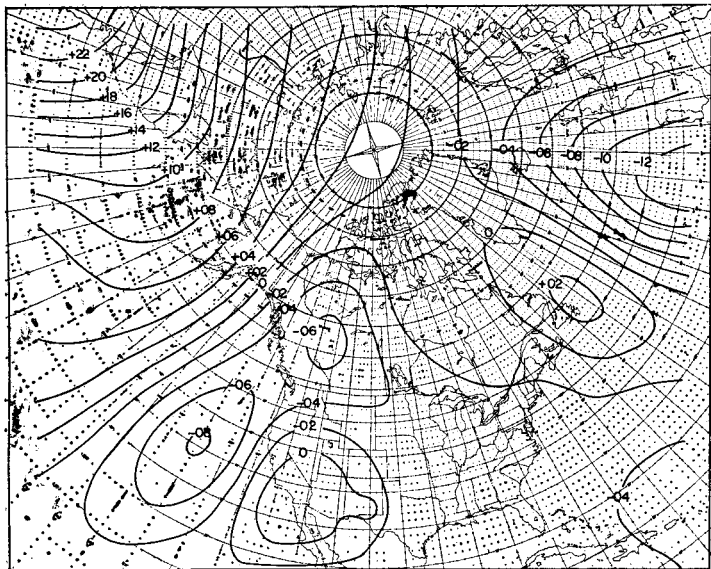


FIGURE 4.—The initial field of $\bar{f}g^{-1}S_1$ at 500 mb. at 0300 GMT April 26, 1956. The irrotational divergent part of the geostrophic velocity vector is equal to the gradient of S_1 , both in magnitude and direction. Contours are labeled in tens of feet.

$$\frac{\partial \bar{S}_2}{\partial s} = \frac{1}{f} \frac{\partial (g\bar{z})}{\partial s} - \frac{\oint \frac{1}{f} \frac{\partial (g\bar{z})}{\partial s} ds}{\oint ds}$$

where s is distance measured counter-clockwise along the boundary. The last term is necessary to close the implied integration, and is quite small, less than one knot. In order to determine the accuracy of the non-divergent part of the geostrophic wind as an approximation to the geostrophic wind itself, equation (9) was solved for \bar{S}_1 . The boundary condition used was

$$\frac{\partial \bar{S}_1}{\partial n} = - \frac{\oint \frac{1}{f} \frac{\partial (g\bar{z})}{\partial s} ds}{\oint ds}$$

where n is distance measured outward and normal to the boundary. Figure 4 shows the field of $\bar{f}g^{-1}\bar{S}_1$, where \bar{f} is the value of the Coriolis parameter at 45° latitude. The largest irrotational wind velocity measured on figure 4 is less than 6 knots. The non-divergent part of the geostrophic wind as given by the stream function, \bar{S}_2 , is therefore nearly the same as the geostrophic wind itself; and equation (8) shows that $\nabla^2 \bar{S}_2$ is a complete accounting of the geostrophic vorticity.²

² In geostrophic barotropic predictions, vorticity is conventionally evaluated without the term $\nabla(gz) \cdot \nabla f^{-1}$. That is, the approximation, $v_z - u_y = f^{-1} \nabla^2(gz)$, is made. To eliminate experimentally this approximation as a possible source of spurious anticyclonogenesis, a prediction was made in which S_2 was computed from the equation $\nabla^2 S_2 = f^{-1} \nabla^2(gz)$. The case was again 0300 GMT April 26, 1956. The result at 36 hours showed even less anticyclonogenesis over the southeastern coast of the United States than the S_2 forecast in figure 5 does. The important point of this article is that any non-divergent estimate of the wind field, within reason, will result in the virtual elimination of the spurious anticyclonogenesis of geostrophic predictions.

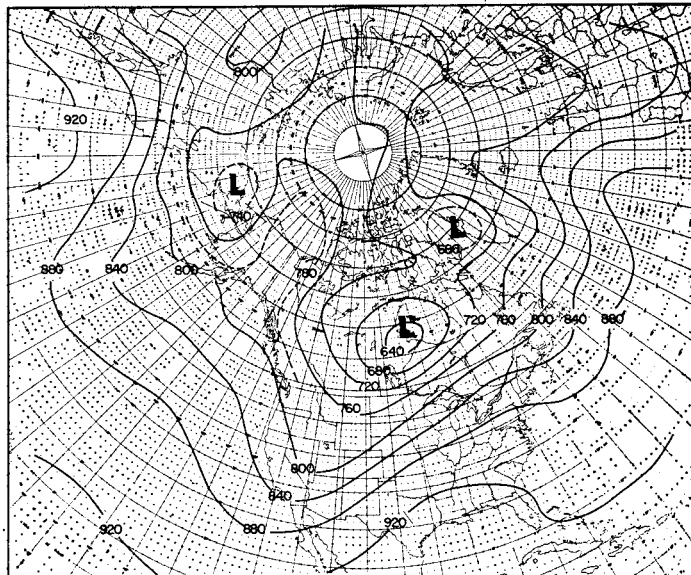


FIGURE 5.—A semi-geostrophic barotropic 36-hour prediction computed from initial conditions at 500 mb. at 0300 GMT April 26, 1956. For prediction purposes the wind field was defined by means of the gradient of S_2 , according to equation (10). Contours are labeled in tens of feet.

Without violating the continuity equation (5), while making use of the empirical facts of near-vanishing pressure tendency at the lower boundary and the quasi-geostrophic nature of atmospheric flow, we may approximate the wind field by means of the stream function \bar{S}_2 .

$$\bar{\mathbf{V}} = -\nabla \bar{S}_2 \times \mathbf{k} \quad (10)$$

A substitution from equation (10) into equation (4); or equivalently, a substitution from equation (10) first into equation (5) and then into equation (6) yields for the barotropic mechanism

$$\frac{\partial}{\partial t} \nabla^2 \bar{S}_2 + J_{z,v} [\bar{S}_2, (K \nabla^2 \bar{S}_2 + f)] = 0 \quad (11)$$

Figure 5 shows a 36-hour prediction of z , according to the system (11). The spurious anticyclonogenesis over the southeastern coast of the United States has indeed been markedly suppressed. Numerical experiments with other cases have verified that the use of \bar{S}_2 to define the flow invariably leads to marked suppression of spurious anticyclonogenesis. The conclusion seems inescapable. Spurious anticyclonogenesis in conventional geostrophic barotropic forecasts arises, in the main, from the violation of the law of conservation of mass implicit in the conventional geostrophic barotropic equations.

3. THE BALANCE EQUATION AND THE BAROTROPIC MODEL

Having derived the equivalent barotropic equations of motion (2) and the equation of continuity (5), and specifying a vanishing pressure change at the lower boundary, in

principle one need not make any further approximations. The three equations (2) and (5) in that circumstance are a complete set in the three unknowns \bar{u} , \bar{v} , and \bar{z} . For convenience we shall replace equation (5) in the set with two equivalent equations relating the velocity components to a fourth unknown, the stream function, $\bar{\psi}$.

$$\begin{aligned}\bar{u} &= -\bar{\psi}_y \\ \bar{v} &= +\bar{\psi}_x\end{aligned}\quad (12)$$

One can now reduce the four equations (2) and (12) to one equation in the one unknown, $\bar{\psi}$. The result is the familiar barotropic equation for non-divergent flow.

$$\nabla^2 \bar{\psi} + J_{x,y}[\bar{\psi}, (K\nabla^2 \bar{\psi} + f)] = 0 \quad (13)$$

In the practice of numerical weather prediction, we do not have observations of $\bar{\psi}$. Both winds and heights of pressure surfaces are observed, but the observed winds are used only as diagnostic information in the analysis of fields of z . Having a field of \bar{z} for initial time, one may treat the four equations (2) and (12) to obtain a single equation relating \bar{z} and $\bar{\psi}$. The result is the balance equation (Petterssen [3], Charney [4], Bolin [5,6], Shuman [7]).

$$f(\bar{\psi}_{xx} + \bar{\psi}_{yy}) - 2K(\bar{\psi}_{xy}^2 - \bar{\psi}_{xx}\bar{\psi}_{yy}) + \bar{\psi}_x f_x + \bar{\psi}_y f_y - g(\bar{z}_{xx} + \bar{z}_{yy}) = 0 \quad (14)$$

Equation (14) differs from previous derivations of the balance equation in the appearance of K , which is a part of the equivalent barotropic equations of motion, but which has been set equal to unity in all of our computations. The geostrophic approximation may thus be entirely avoided, except perhaps in lateral boundary conditions for the solution of equation (14), and then only in integrations over limited areas of the earth.

Upon integrating the balance equation (14), one finds that the validity of the geostrophic wind as an approximation is upheld. Figure 6 shows the difference between $\bar{f}g^{-1}\bar{S}_2$ and $\bar{f}g^{-1}\bar{\psi}$. In areas of small gradients of $\bar{f}g^{-1}\bar{S}_1$ in figure 4, the quantity displayed in figure 6 may be considered as a scaled stream function of the ageostrophic component of the "balanced" wind. In any case, \bar{S}_1 and the difference between \bar{S}_2 and $\bar{\psi}$ may be simply combined to determine the ageostrophic component of the "balanced" wind. It is to be noted that the ageostrophic wind from figure 6 is, in its general level, an order of magnitude smaller than the geostrophic wind of figure 1.

In the solution displayed in figure 6, the most pronounced feature is the large-scale circulation about the center of the chart. This is to be expected, because of the cyclostrophic effects of the mean circumpolar flow and other net cyclonic conditions in the atmosphere. However, in an integration over the entire earth, or over a hemisphere, the center of the ageostrophic circulation would undoubtedly be near the pole. The shift of the

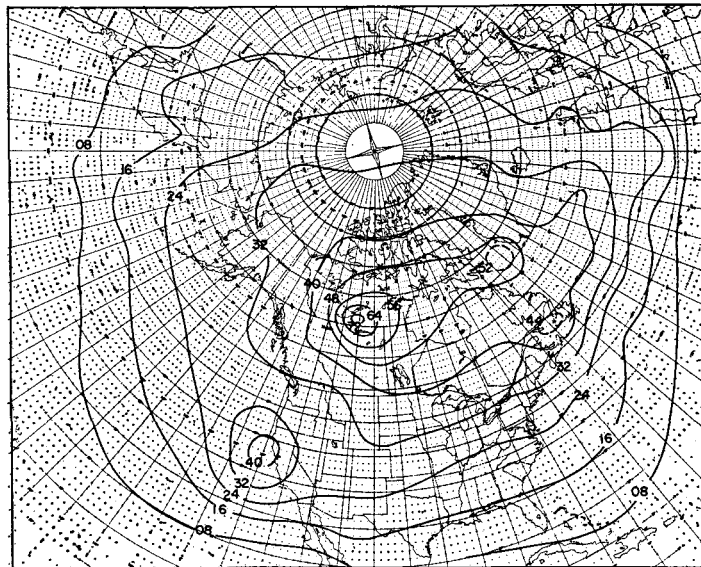


FIGURE 6.—The field of the difference $\bar{f}g^{-1}(\psi - S_2)$ at 500 mb. at 0300 GMT April 26, 1956. ψ was computed from the balance equation (14) using the 500-mb. heights for z . S_2 was computed from equation (8). Contours are labeled in tens of feet.

center of circulation toward the center of the chart is forced by the boundary condition used in the computation

$$\frac{\partial \bar{\psi}}{\partial s} = \frac{1}{f} \frac{\partial g \bar{z}}{\partial s} - \frac{\oint \frac{1}{f} \frac{\partial g \bar{z}}{\partial s} ds}{\oint ds}$$

With inflow arbitrarily set to very nearly geostrophic values, the ageostrophic component of the balanced wind near the boundary is forced to be nearly tangent to the boundary, and the center of any net circulation otherwise about the pole is forced away from the pole toward the center of the chart. This should not be very damaging to the calculation of the ageostrophic wind over the United States in our grid, but on the Asian side of the grid the calculated ageostrophic wind cannot be expected to bear any resemblance to reality. The most obvious remedy for this is a calculation on a hemispheric grid, which is at present being carried out by the JNWP Unit.

With reservations concerning the boundary errors discussed above, differences between predictions made with balanced ($\bar{\psi}$) winds and semi-geostrophic (\bar{S}_2) winds must be due to the inconsistencies between the initial \bar{S}_2 wind and the initial field of \bar{z} , in terms of the equivalent barotropic balance equation (14). Figure 7 shows a prediction made with $\bar{\psi}$ computed initially from equation (14). Comparing figures 5 and 7 we find that the residual spurious anticyclonogenesis of the prediction made with \bar{S}_2 winds has been eliminated by bringing the initial wind field into correspondence with the initial \bar{z} field in an equivalent barotropic sense. Sufficient comparisons of this kind have not yet been made to determine the degree of universality of the improvement of balanced predictions

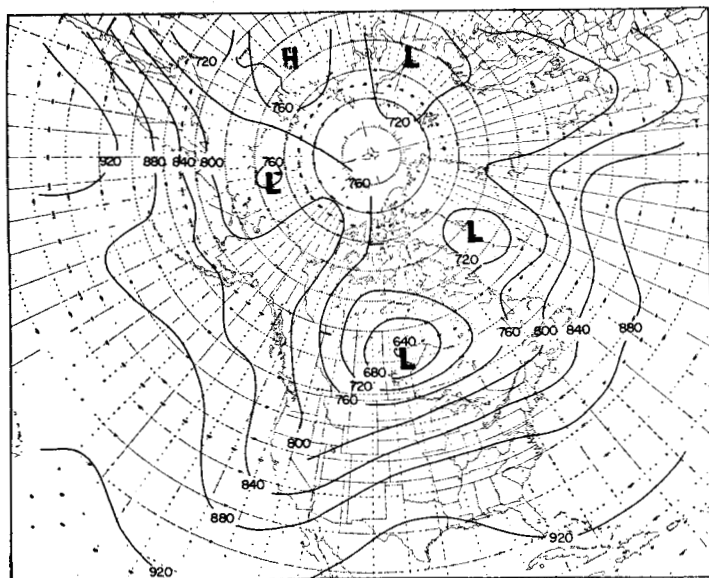


FIGURE 7.—A balanced barotropic 36-hour prediction computed from initial conditions at 500 mb. at 0300 GMT April 26, 1956. For prediction purposes the wind field was defined by means of the stream function, ψ , computed from the balance equation (14). Contours are labeled in tens of feet.

over semi-geostrophic (\bar{S}_2) predictions. Such comparisons, in any event, will not be conclusive until they are carried out on a hemispheric grid.

4. CONCLUDING REMARKS

Since April 20, 1956, the Joint Numerical Weather Prediction Unit has been computing balanced barotropic 72-hour predictions on a daily basis over the area shown in the figures illustrating this article. Equations (13) and (14) are the basis of the daily operational barotropic computations. In comparisons which have been made with conventional geostrophic barotropic predictions, it has been found that in some cases the two systems yield predictions of comparable accuracy, but in many cases the spurious anticyclogenesis of the geostrophic predictions is disastrous. Such errors are characteristically associated with weather regimes, so that they may appear day after day for a week or more, rendering numerical predictions useless for a like period.

The results of this study in hand may be summarized by saying that the use of a slightly modified geostrophic wind, which is strictly non-divergent, leads to a dramatic improvement over conventional geostrophic predictions. Use of winds calculated from the balance equation, on the other hand, yields a much less marked improvement over predictions made with semi-geostrophic non-divergent

wind fields. It can be logically induced that the primary benefit of balanced winds, as opposed to geostrophic winds, is not, as has been suggested in the literature, due to dynamic effects inherent in the balance equation, but is due to the fact that they satisfy the law of conservation of mass.

Ramifications of the predictive consequences discussed here extend beyond the barotropic model. Proposed baroclinic models until very recently have generally made free use of the geostrophic approximation, while assuming vanishing surface pressure tendencies at the lower boundary. There is no theoretical reason to believe, and indeed there is abundant empirical evidence (Cressman and Hubert [8]) to deny, the thesis that baroclinic models are less sensitive to the violation of the law of mass conservation implied in the direct use of the geostrophic wind.

ACKNOWLEDGMENTS

Full acknowledgments would read like a personnel roster of the Joint Numerical Weather Prediction Unit. Only within such an organization could this study have been completed, depending as it does on inspiration and ideas from associates, professional skills of both meteorologists and mathematicians, long series of cases to inspect, and routine work of drafting and typing. I would especially single out for expressions of gratitude Dr. George P. Cressman, who very early understood the importance of the problem treated, and who lent directional assistance during the search for the underlying causes and solution.

REFERENCES

1. J. Charney, "On the Physical Basis for Numerical Prediction of Large-Scale Motions in the Atmosphere," *Journal of Meteorology*, vol. 6, No. 6, Dec. 1949, pp. 371-385.
2. J. Charney, "The Dynamics of Long Waves in a Baroclinic Westerly Current," *Journal of Meteorology*, vol. 4, No. 5, Oct. 1947, pp. 135-162.
3. S. Petterssen, "On the Relation between Vorticity, Deformation, and Divergence, and the Configuration of the Pressure Field," *Tellus*, vol. 5, No. 3, Aug. 1953, pp. 231-237.
4. J. Charney, "The Use of the Primitive Equations of Motion in Numerical Prediction," *Tellus*, vol. 7, No. 1, Feb. 1955, pp. 22-26.
5. B. Bolin, "Numerical Forecasting with the Barotropic Model," *Tellus*, vol. 7, No. 1, Feb. 1955, pp. 27-49.
6. B. Bolin, "An Improved Barotropic Model and Some Aspects of Using the Balance Equation for Three-Dimensional Flow," *Tellus*, vol. 8, No. 1, Feb. 1956, pp. 61-75.
7. F. Shuman, "A Method for Solving the Balance Equation," *Technical Memorandum No. 6*, Joint Numerical Weather Prediction Unit, 1955, 12 pp.
8. G. Cressman and W. E. Hubert, "A Study of Numerical Forecasting Errors," *Monthly Weather Review*, vol. 85, No. 7, July 1957, pp. 235-242.